Conformational analysis of the endogenous μ-opioid agonist endomorphin-1 using NMR spectroscopy and molecular modeling

Brent L. Podlogar[1,a], M. Germana Paterlini[b], David M. Ferguson[2,b], Gregory C. Leo[a], David A. Demeter[a], Frank K. Brown[a], Allen B. Reitz[a]

[a]*Department of Medicinal Chemistry, The R.W. Johnson Pharmaceutical Research Institute, Route 202, P.O. Box 300, Raritan, NJ 08869, USA*
[b]*Department of Medicinal Chemistry, University of Minnesota, 308 Harvard St. SE, Minneapolis, MN 55455, USA*

Received 6 August 1998

Abstract Endomorphin-1 (Tyr-Pro-Trp-Phe-NH_2) is a highly selective and potent agonist of the μ-opioid receptor. To identify structural attributes unique to this opioid peptide and potential sites of recognition, a conformational analysis has been performed using multidimensional NMR and molecular modeling techniques. The spectroscopic results, derived from experiments in both DMSO and water, indicate that endomorphin-1 exists in the *cis*- and *trans*-configuration with respect to the Pro-omega bond in approximately 25% and 75% populations, respectively. In DMSO, the *cis*-configuration adopts a compact sandwich conformation in which the Tyr and Trp aromatic rings pack against the proline ring, whereas the *trans*-configuration adopts an extended conformation. Although non-random structure was not observed in water, condensed phase molecular dynamics calculations indicate that *trans*-isomers dominate the population in this higher dielectric medium. Structural comparison of the *cis*- and *trans*-configurations with morphine and selective μ-peptide ligands PL-017 and D-TIPP, as well as the δ-selective peptide ligands TIPP (δ-antagonist, μ-agonist) and DPDPE were also performed and suggest the *trans*-isomer is likely the bioactive form. A hypothesis is proposed to explain μ- and δ-selectivity based on the presence of spatially distinct selectivity pockets among these ligands.

Key words: Opioid; Peptide structure; Conformational analysis; Molecular dynamics; Multidimensional nuclear magnetic resonance spectroscopy; Structure-activity relationship

1. Introduction

Opioid receptors are important targets for pharmacological interaction in acute pain therapy [1]. Recent work in this area appears to indicate that the observed effects of many opioid analgesics are caused by combinations of opioid receptor type activation [2–5]. To unravel these interactions, detailed structural models capable of differentiating δ, μ and κ receptor type selectivity and ultimately, receptor activation vs. inactivation are crucial. Structural models have been generally derived from small molecule opioid receptor agonists and antagonists [6,7], and while they have advanced our thinking in this area, and have shed some light on separation of δ binding from κ and μ binding [8], they are neither predictive nor complete. Although the small molecule ligands, e.g. opiate alkaloids, are less problematic to model, their small physical size as compared to the endogenous opioid ligands, e.g. enkephalins, endomorphins, dynorphins, restricts ligand interactions to a small region of the receptor active site and may fail to fully address the full complement of interactions responsible for specific receptor type activation [9,10]. Identification and structural characterization of selective opioid peptide ligands for the δ receptor (e.g. DPDPE [11], JOM-13 [12]) and the κ receptor (dynorphin [13,14]) have allowed modeling studies to begin for these types, but to date, few such studies for μ-selective peptide ligands (D-TIPP-NH_2) have been reported [15].

Recently, two novel peptides, endomorphin-1 (YPWF-NH_2) and endomorphin-2 (YPFF-NH_2) were reported as the endogenous μ receptor ligands [16]. Endomorphin-1 shows remarkable affinity for the μ receptor (360 pM) and selectivity of 4000- and 15 000-fold for the μ receptor over the δ and κ receptors, respectively. The availability of the endomorphin peptides makes possible the comparison with other μ-selective peptides, such as D-TIPP (Y-D-Tic-FF-NH_2) [15] and PL-017 (YPF-D-P-NH_2) [17]. We have studied the properties of endomorphin-1 using NMR spectroscopy and molecular simulations, and the results have been complemented with molecular comparisons of this peptide with D-TIPP and PL-017. Structural comparisons with the δ-agonist DPDPE [11] and the dual μ-agonist/δ-antagonist, TIPP-NH_2 [18] have also been performed to rationalize structure-based selectivities among these ligands and opioid receptor types.

2. Materials and methods

2.1. Synthesis of endomorphin-1

Endomorphin-1 was synthesized using the Merrifield solid-phase method of peptide synthesis. t-BOC chemistry with HBTU [2-(1H-benzotriazol-1-yl)-1,1,3,3-tetramethyluronium hexafluorophosphate] activation was employed for peptide elongation. The peptide-resins were treated with 95% HF/5% anisole at −4°C for 1.5 h to generate free peptides. The peptide-associated resin complexes were washed with dimethyl ether to remove the anisole. The peptides were extracted in 20% HOAc and purified on two 22.5×250 mm Vydac C18 columns in tandem (5 μm particle size, 300 Å pore size) using a gradient of 0–27% 'B' in 27 min at a flow rate of 30 ml/min. The 'A' buffer was 0.1% TFA/water and the 'B' buffer was 0.1% TFA/acetonitrile. The fractions containing the desired peptide were then combined and lyophilized. The dried peptides were characterized by analytical RP-HPLC and electrospray MS.

2.2. NMR spectroscopy

All spectra were recorded at 600.13 MHz on a Bruker DMX spectrometer. Samples in water included 10% deuterium oxide as the lock solvent and TSP as the chemical shift reference. Spectra were recorded at 275 K or 278 K. Sample concentrations used were approximately

[1]Corresponding author. Current address: Bayer Corp., 400 Morgan Lane, West Haven, CT 06516, USA.
E-mail: bpodloga@prius.jnj.com

[2]Corresponding author.
E-mail: ferguson@quinn.medc.umn.edu

0014-5793/98/$19.00
PII: S0014-5793(98)01202-2

0.6 mM or 3.5 mM. TOCSY spectra were measured using a 50 ms spin lock (10 000 Hz field strength) using either DIPSI-2 [19] or MLEV-17 [20] and magic angle gradient water suppression with the 3-9-19 Watergate sequence [21,22]. Through-space correlations were detected using both NOESY, [23] ROESY [24] (2550 Hz field strength) and off-resonance ROESY [25] (10 000 Hz field strength, 10 000 Hz off-resonance) experiments using mixing times ranging from 150 ms to 250 ms. Water suppression was accomplished using magic angle gradient 3-9-19 Watergate or low power, continuous wave pre-saturation. The sample in DMSO-d_6 was approximately 7 mM and TMS was used as the chemical shift reference. TOCSY [26] (10 000 Hz spin lock field for 60 ms) and NOESY (250 ms mix time) spectra were recorded at 297 K. All 2D spectra were acquired in the phase sensitive mode (States-TPPI) and processed using a 90° shifted, squared sine-bell apodization [27].

2.3. Restrained molecular dynamics

Restrained molecular dynamics simulations were conducted using the Insight II/Discover 95 suite of software. All simulations were conducted in vacuo using the CFF91 forcefield[3]. The NOE distance data were applied a generic distance constraints using a lower distance bound of 1.8 Å, and a force constant value set to 10 kcal/mol Å^2. No distance cutoffs were used; a distance dependent dielectric of $3.5\times r$ was used. A 20 ps high temperature molecular dynamics simulations (700°C) was used to generate a total of 200 random starting geometries. The random structure were cooled by successive minimizations with the forcefield scaled at 0.5 (500 cycles of steepest descents); 0.75 (500 cycles of steepest descents), 1.0 (1000 cycles of steepest descent followed by 1500 cycles of conjugate gradient minimization; convergence criterion set to 0.1 kcal/Å.) All ω bonds were forced to 180° (or 0° for the *cis*-proline isomer) using a force constant of 100 kcal/Å^2. Chiral centers were constrained to the starting values.

2.4. Systematic conformational searching

General molecular modeling and conformational analysis was conducted in Sybyl 6.3[4]. Atomic point charges were calculated using the Gasteiger-Hückel method [28–32]. Full geometry optimizations were done using the Tripos force field [33,34] with the Powell minimizer and electrostatics. The following variable parameters were set: termination_criterion = energy, min_energy_change = 0.00001 kcal/mol, max_iterations = 1 000 000, dielectric_constant = 2.0, dielectric_function=distance. Default settings were used for all other variable parameters.

Systematic conformational searches were done using the Tripos force field with the csearch algorithm, energies, and electrostatics. All rotatable bonds were searched from 0° to 359°. An angle increment of 10° was used for the Tyr ψ dihedral, 20° for the Tic ψ dihedral, and 10° for all the backbone and sidechain rotatable bonds in the two Phe residues for a total of 10 rotatable bonds. The following variable parameters were set: reference_conformation = zeroed, van_der_Waals_scaling_factors (general = 0.90, 1–4 = 0.82, hbond = 0.65), energy_cutoff = 9999.9 kcal/mol, dielectric_constant = 2.0, dielectric_function = distance. Default settings were used for all other variable parameters.

Potential energy surface analyses were done in PESA 1.0 [35]. The following variable parameters were set: find minima, neighbors minima noprint, statistics surface minima. Default settings were used for all other variable parameters.

Steric and electrostatic CoMFA fields [36–38] were calculated with the CoMFA regions defined automatically using the molecular volumes option. Default settings were used for all other variable parameters. Field correlations were calculated with the QSAR COMFA FIELD COMPARE command. The correlation coefficients of the steric and electrostatic fields were summed and the conformer with the highest value was selected as the most similar. This conformer was then minimized as described above and was fit to *trans*-endomorphin-1.

2.5. Molecular dynamics simulations

MD simulations were performed using the Amber 4.1 suite of programs with the Cornell et al. force field [39]. Simulations in aqueous solutions were obtained by placing endomorphin-1 in a box of equilibrated water and then stripping any water molecule at a distance of 2.0 Å or less from the peptide. The dimensions of the water box were $46\times38\times35$ for a total of 1647 water molecules. An energy minimized, extended structure was used as the starting structure. Molecular dynamics simulations were conducted at constant temperature and pressure using the Berendsen coupling scheme with a time constant of 0.2 for temperature and pressure regulation. Bond lengths were constrained using the SHAKE algorithm and an integration time step of 2 fs was used. A 10 Å cutoff was used for non-bonded interactions and the non-bonded pairlist was updated every 50 fs. Equilibrium was reached after about 600 ps as judged from the rmsd deviation from the initial structure which rose to 4.5 Å.

3. Results

NMR experimentation was conducted using standard techniques (see Section 2) in H_2O (4°C) and in DMSO-d_6 (25°C). A variable temperature study was also conducted in DMSO-d_6 to evaluate internal hydrogen bonding. The 1D spectrum of endomorphin-1 (Fig. 1) clearly highlights the existence of *cis*- and *trans*-isomer populations.

The relative peak intensities from the 1D spectrum for both the aqueous and DMSO media indicate that endomorphin-1 resides in 25/75% populations of the *cis*-*trans* isomers.

The *cis*-*trans* peak assignments were confirmed by the characteristic sequential NOEs between the Pro and Tyr residues [40]. Non-sequential ROESY cross peaks were not observed in aqueous solution for endomorphin-1.

For the *cis*-isomer in DMSO (Fig. 2), NOE cross peaks between Pro and both the $Tyr_{2,6}$ and $Tyr_{3,5}$ protons, and the Trp aromatic protons were observed, and are indicative of a stabilized packing arrangement of the aromatic side chains with the proline ring. The *trans*-isomer also exhibited some elements of non-random conformation, although the high degree of overlap caused by the close chemical shifts observed for $Trp_{\beta2}$ and $Tyr_{2,6}$ (7.060 and 7.055 ppm, respectively) makes unambiguous assignments difficult. NOE cross peaks between the $Tyr_{2,6}$ aromatic protons and the Pro δ and β protons suggest that the Tyr may pack against the Pro as in the case for the *cis*-isomer. In contrast, no cross peaks implicating a stabilized packing interaction between the Pro and Trp or between Trp and Phe for the *trans*-isomer are observed[5]. Additionally, the presence of an NOE cross peak between the Phe aromatic protons and the Pro β protons suggests the tendency for the *trans*-isomer to adopt an extended conformation characterized by alternating sidechains for the Trp and Phe region. Variable temperature NMR experiments show no evidence for internal hydrogen bonding for either the *cis*- or *trans*-isomer. Conformational forms characterized by stable turn conformation in both isomers can therefore be eliminated.

The NMR data yield too few NOE constraints per residue

[3] INSIGHT/DISCOVER: Biosym Technologies, 9685 Scranton Road, San Diego, CA 92121-2777, USA. Discover 95 utilizes the CVFF forcefield: Dauber-Osguthorpe, P., Roberts, V.A., Osguthorpe, D.J., Wolff, J., Genest, M. and Hagler, A.T. (1988) Proteins Struct. Funct. Genet. 4, 31–47, and references therein.

[4] Tripos Associates, 1699 S. Hanley Road, Suite 303, St. Louis, MO 63144, USA.

[5] At the reviewer's suggestion, the cross peak labeled $Tyr_{2,6}$-$Pro_{\delta2}$ was confirmed by peak-shape analysis to be devoid of any W_2 contribution. Since no W_2-$P_{\delta2}$ cross peak was observed (at ~3.5 ppm), we concluded that the overlapped region about ~3.0 ppm has little or no contribution from W_2-$P_{\delta1}$.

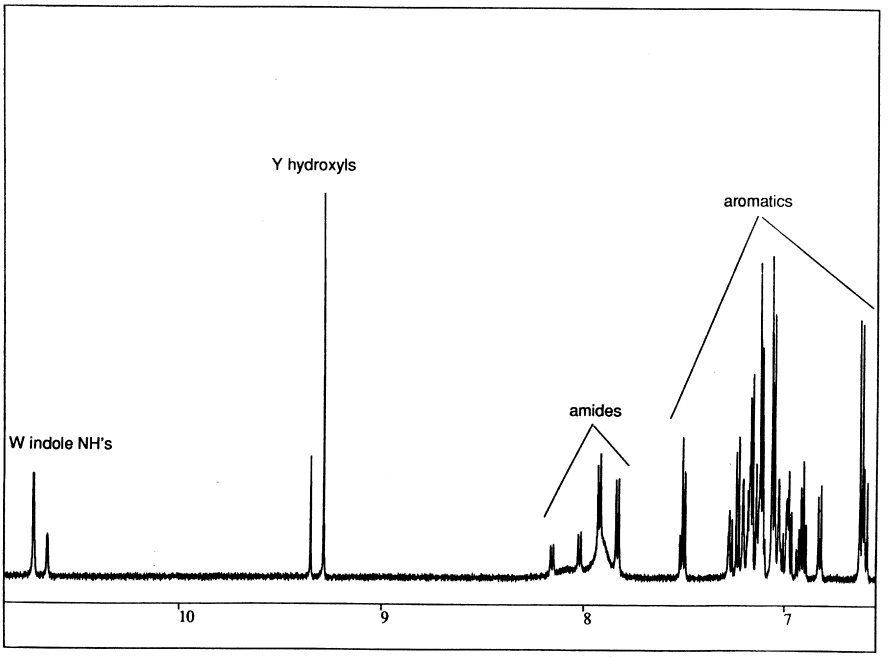

Fig. 1. 1D NMR spectrum of endomorphin-1 in DMSO-d_6 (3.5 mM, 25°C).

for a rigorous structure determination. Nevertheless, application of the observed cross peaks via restrained molecular dynamics was conducted to obtain plausible 'NMR structures' for our modeling studies that reflect the conformations which cannot be ruled out by the NMR data. Low energy conformations consistent with the NMR data were determined using NOE restraints for both the *cis*- and *trans*-isomers. A total of 19 NOE restraints from the *cis*-isomer, and 10 NOE restraints from the *trans* isomer were taken from the NOESY spectra. The restraints were calibrated to internal stationary backbone proton-proton distances (*trans*-Tyr_N-Pro_β and *trans*-Phe_N-Pro_β) and are shown in Tables 1 and 2.

High temperature molecular dynamics (see Section 2) was used to generate a set of diverse starting conformations to which the NOE constraints were gradually applied. Representative low energy structures with no NOE violations for the *cis*-isomer are shown in Fig. 3. In the overlay, a compact sandwich conformation is clearly discernible, created by the packing of Tyr and Trp around the proline residue. Fig. 4 shows a representative low energy structure for the *trans*-isomer.

Table 1
cis-YPWF-NH_2 NOESY analysis. DMSO at 25°C

NOE pair	Estimated distance (Å)
W_2 W_α	4.2
W_2 $P_{\delta 2}$	5.0
$Y_{2,6}$ $P_{\delta 1}$	4.6
$Y_{3,5}$ P_β	4.6
F_{NH} $W_{\beta 2}$	3.8
$Y_{2,6}$ P_β	4.6
W_2 P_β	5.0
W_{NH} P_β	3.4
$Y_{2,6}$ P_α	3.8
W_{NH} P_α	2.6
$Y_{2,6}$ Y_β	2.6
W_{NH} Y_α	3.8
W_β W_2	3.8
$Y_{3,5}$ Y_β	4.6
F_{NH} W_α	2.6
W_{NH} W_α	3.8
F_{NH} F_β	3.8
F_{NH} P_β	5.0
F_{NH} Y_α	4.6

4. Discussion

One of the key questions this study raises regards the bioactive conformation of endomorphin-1. Although the NMR data point to the existence of two very distinct structures of this small peptide, it is highly unlikely that both isomers shown in Figs. 3 and 4 bind the μ receptor with high affinity. In previous work on related peptide structures, *cis*-isomers similar to that shown in Fig. 3 have been shown to be structurally important in defining the bioactive conformation; the YP-Ar motif displayed by endomorphin-1 (where Ar is an aromatic residue) is also found in immunogenic peptides from the influenza virus hemagglutinin and the insect kinin neuropeptides [41,42]. NMR studies of those YR-Ar peptides have shown that the *cis*-isomer is highly stabilized by the formation of a reverse turn in solution. The Tyr and Trp sidechains of endomorphin-1 pack against the proline ring in a similar fashion as those of the immunogenic peptides,

Table 2
trans-YPWF-NH_2 NOESY analysis. DMSO at 25°C

NOE pair	Estimated distance (Å)
$F_{2,6}$ P_β	5.0
$Y_{2,6}$ P_β	4.2
W_4 W_β	3.4
W_4 W_α	3.4
$Y_{2,6}$ $P_{\delta 1}$	2.6
$Y_{2,6}$ $P_{\delta 2}$	3.4
$Y_{2,6}$ Y_α	2.6
W_{NH} $P_{\beta 1}$	3.4
F_{NH} $P_{\beta 1}$	3.8
F_{NH} $P_{\beta 2}$	5.0

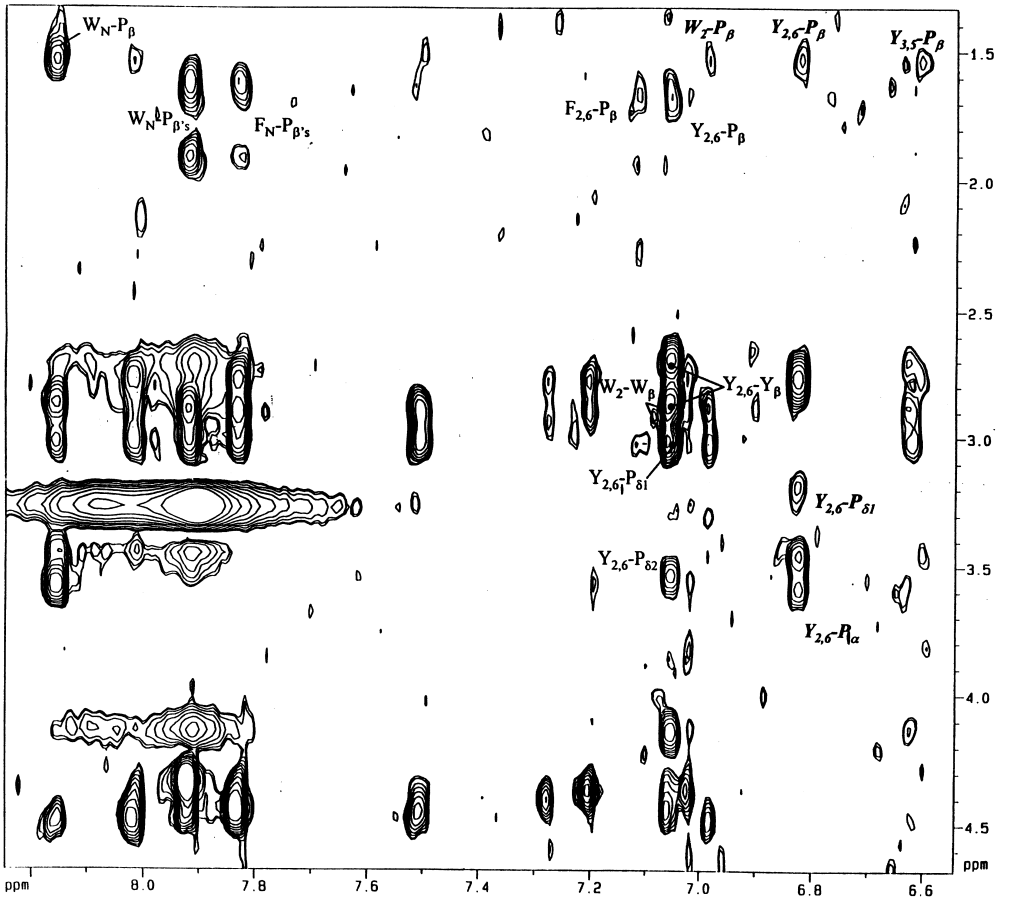

Fig. 2. NOESY spectrum of YPWF-NH_2 in DMSO-d_6 (3.5 mM, 25°C, 250 ms mixing time). Cross peaks corresponding to the *cis*-isomer are italicized. Sequential NOEs exhibit from ~50:1 to ~80:1 signal to noise ratio. All NOEs considered exhibited >3:1 signal to noise ratio.

but endomorphin-1 is devoid of hydrogen bonds as indicated by the NMR temperature studies. This may explain why the *cis*-isomer is present in 70% for the immunogenic peptides versus the 25% observed here for endomorphin-1.

The structural properties of *cis*-endomorphin-1 were further

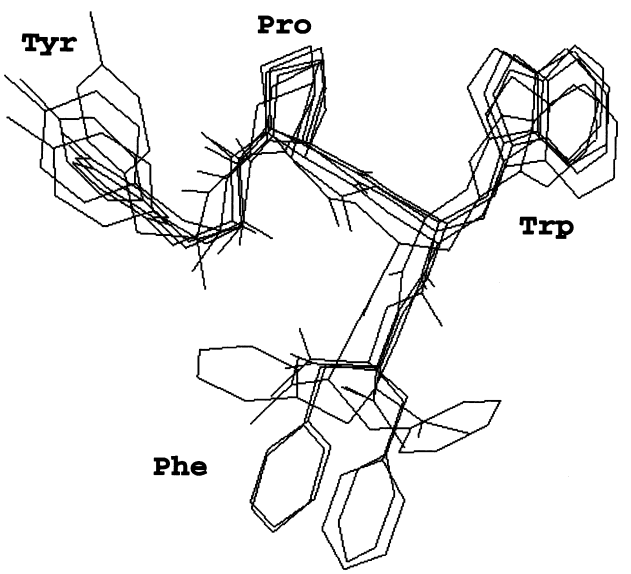

Fig. 3. Low energy *cis*-conformations consistent with DMSO NOE data. Structures are aligned using an RMS fit of the C_α carbons.

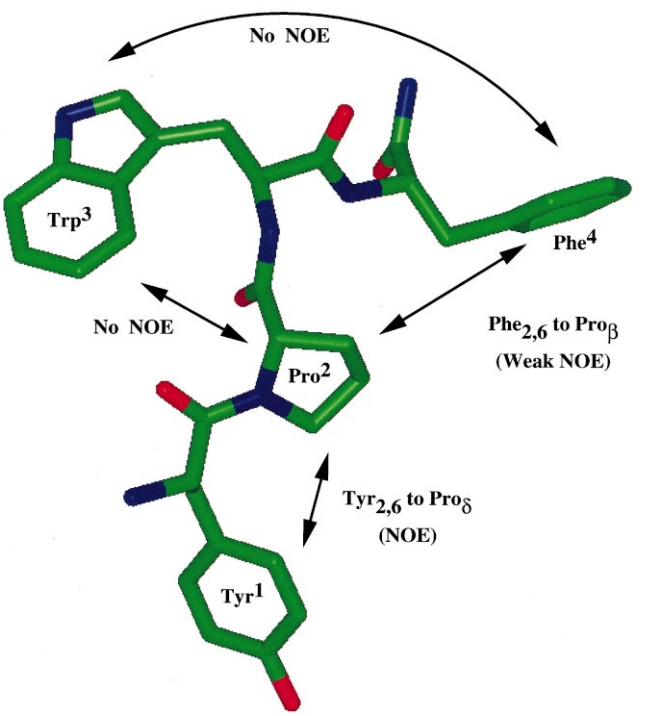

Fig. 4. Low energy *trans*-conformation consistent with DMSO NMR data. Absence of NOE cross peaks between Pro^2 and Trp^3 as well as Trp^3 and Phe^4 support extended conformation.

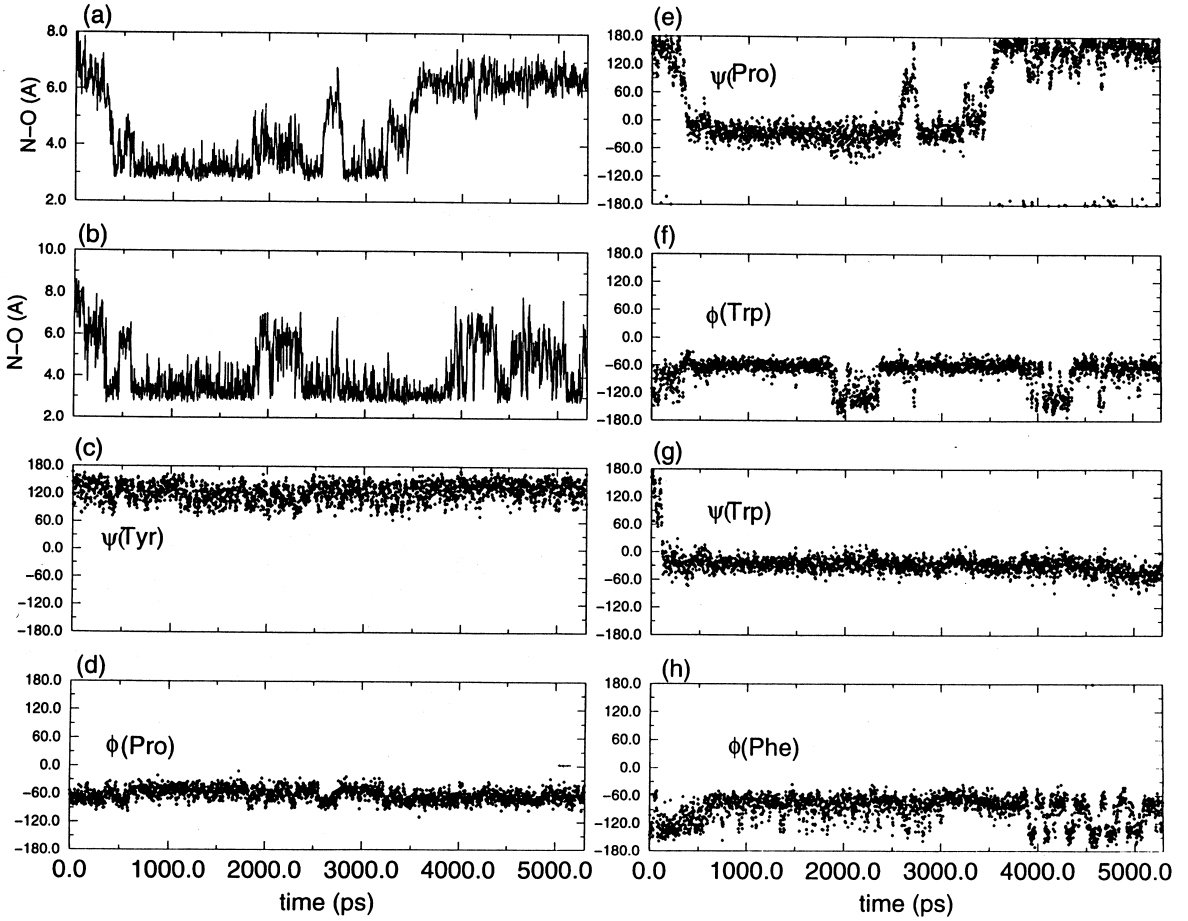

Fig. 5. Timecourse of a 5 ns simulation of solvated endomorphin-1. Equilibration was reached after 600 ps, as monitored by the RMS deviation from the initial structure. a: H-bonding distance between the carboxylic oxygen of Tyr and the amide nitrogen of Phe. b: H-bonding distance between the carboxylic oxygen of Pro and the terminal amide nitrogen. c–h: Timecourse of the backbone dihedrals.

explored using molecular dynamics simulations in water and in vacuo with varying dielectric constants. In each case, the simulations failed to reproduce the sidechain packing interactions predicted by our NOE data and observed in published reports [41,42]. Since the dielectric properties of DMSO and liquid water are significantly different (40 versus 78.5, respectively), this result is not surprising. Temussi et al. have also reported viscosity effects on the structure of small peptides [43]. Similar to our results, they observed a pattern of structure in DMSO and no structure in aqueous mediums. Since structural elements were observed only in DMSO, which is not a biologically relevant solvent, and that only 25% of the peptide population for endomorphin-1 exists in the *cis*-form, we conclude that the compact structure observed for the *cis*-isomer is an artifact of the solution conditions.

To investigate the significance of the *trans*-isomer to peptide binding, molecular dynamics simulations have also been performed on this conformer in water. An analysis of a 5 ns trajectory reveals the peptide exists in two stable structural families separated by a set of rotations about the ψ (Pro)

Table 3
Torsion angles of the NMR and simulated structures of endomorphin-1 and of the peptides used in the structural comparison[a]

Peptide[b]	X_0	X_1	X_2	Tyr		X_0			X_1			X_2		
				ψ	χ_1	ϕ	ψ	χ_1	ϕ	ψ	χ_1[c]	ϕ	ψ	χ_1[c]
cis-Endomorphin-1 NMR structure	Pro	Trp	Phe	139	−176	−74	172	33	−76	0	−48	−80	−120	−179
trans-Endomorphin-1 NMR structure	Pro	Trp	Phe	154	−64	−77	180	33	−106	−179	−39	−50	112	−179
trans-Endomorphin-1 'β-III-like' structure	Pro	Trp	Phe	120	−60	−70	−30	33	−60	−30	g^+	−60	d	t,g^+,g^-
trans-Endomorphin-1 'extended' structure	Pro	Trp	Phe	150	−60	−70	150	33	−120	−30	g^+, t	−150	d	t,g^+,g^-
trans-PL-017	Pro	*N*-MePhe	D-Pro	154	−68	−74	165	33	−130	63	−61	60	114	25
D-TIPP	D-Tic	Phe	Phe	148	−59	99	−165	−58	58	50	−47	−48	111	174
L-TIPP-NH_2	L-Tic	Phe	Phe	151	−65	−95	−174	63	−137	65	−55	−153	110	179

[a]Angles are in degrees.
[b]Peptides are denoted according to the general sequence Tyr-X_0-X_1-X_2-NH_2.
[c]t = trans ($\chi_1 = 180$), g+ = gauche+ ($\chi_1 = 60$), g^- = gauche− ($\chi_1 = -60$).
[d]Conformations with either $\psi = -90$ and $\psi = -120$ were found.

and ϕ (Trp) dihedral angles (Fig. 5 and Table 3). One family of states is similar to the β-III turn and is observed between 0.5 and 1.8 ns and again between 2.5 and 3 ns. During these intervals in time, Pro is in the α-conformation with hydrogen bonds occurring between the Tyr-carbonyl and the Phe-NH groups. An additional hydrogen bond can also form between the Pro-carbonyl and the terminal amine group in this compact structural form as shown in Fig. 5. After 3 ns, however, the peptide reverts to an extended form devoid of hydrogen bonds. This second conformational family is characterized by having relatively extended dihedral angles of 150° and −120° for ψ (Pro) and ϕ (Trp), respectively.

Although our molecular dynamics time lengths are insufficient to determine the statistical probability of these two families occurring, the extended structure is consistent with the NOE data of the *trans*-isomer. In comparing the experimental and calculated structures of *trans*-endomorphin-1, similar backbone dihedral angles are evident, but differences are seen in the sidechain conformations. While the NMR data are compatible with either the Tyr sidechain packed against the Pro ($\chi_1 \sim -150°$) or away from Pro ($\chi_1 \sim -60°$), Tyr χ_1 maintained a gauche (−) (χ_1 −60°) throughout the simulation.

To settle this apparent inconsistency, we have capitalized on the observation that many potent δ, μ and κ opioid ligands possess a tyramine (*para*-hydroxy phenethylamine) moiety buried within their molecular framework. In fact, the tyrosine ring and the positively charged nitrogen are general requirements for nearly all of the reported small molecule pharmacophores [6]. Therefore, in our comparisons, we require that the tyramine moiety of the peptide ligands adopt the conformation as defined by the small molecule ligands such as morphine.

Our use of the extended conformation of *trans*-endomorphin-1 for the bioactive conformation becomes justified when considering how it overlays with other selective μ ligands, PL-017 and D-TIPP. PL-017, by virtue of its two proline rings and *N*-methyl amide, prohibits internal hydrogen bonding, is conformationally restricted and is essentially forced to adopt an extended conformation[6,7]. Given its restricted conformational flexibility, it was used as a reference template for an active analog modeling approach [44]. Complimentary fit of valid *trans*-endomorphin-1 structures was accomplished with minimal modification about the Phe residue to align the C-terminus. Alignment of D-TIPP with *trans*-endomorphin-1 presented greater difficulty because its D-amino acid at the 2-position prevented direct correspondence with endomorphin-1 and PL-017 in this region. We therefore conducted a systematic conformational search of D-TIPP to map its potential energy surface. A total of 491 local minima were identified on the potential energy surface [35] and were aligned to *trans*-endomorphin-1 using the 'tyramine' moiety and the ring centroids of residues 3 and 4 as pharmacophore features. The D-TIPP conformer most similar to *trans*-endomorphin-1 was then selected by calculating the maximum correlation of their steric and electrostatic CoMFA fields with those derived for endomorphin-1 [36–38]. A composite overlay of this D-TIPP conformer with *trans*-endomorphin-1 and PL-017 is shown in Fig. 6.

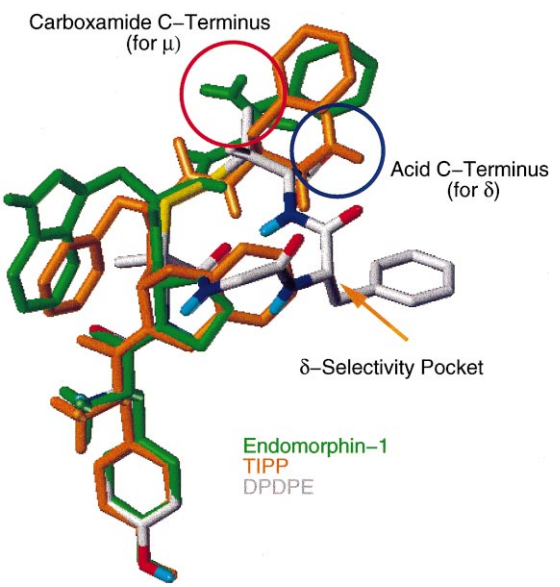

Fig. 6. Comparison of *trans*-endomorphin-1 'extended conformation' with D-TIPP-NH_2 and PL-017.

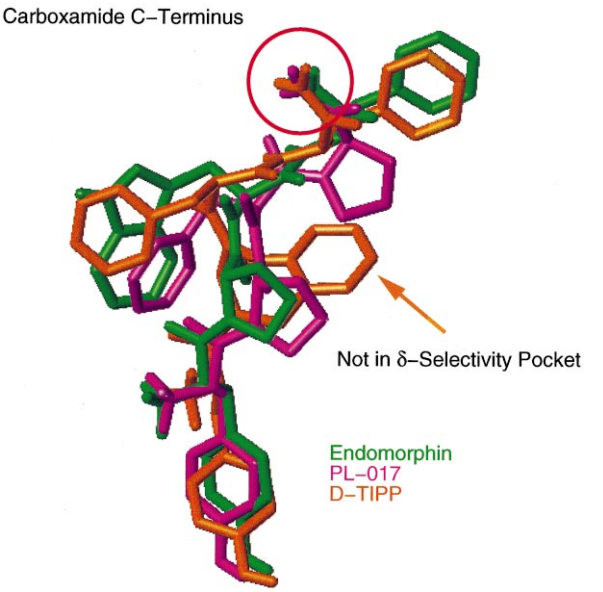

Fig. 7. Comparison of *trans*-endomorphin-1 'extended conformation' with DPDPE and TIPP-NH_2.

As seen in Fig. 6, all three peptides are anchored at the tyrosine residue in accordance with a good fit in this region with small molecule ligands. The hydrophobic groups, Trp^3, Phe^3 and Phe^3 for endomorphin-1, PL-017 and D-TIPP, respectively, all occupy a region of space which we propose as the μ-selectivity region. This is to be contrasted to the δ-selectivity region as identified by Portoghese et al. [8] and Loew et al. [6], also indicated in Fig. 6.

---

[6] Note added in proof, see: Wilkes, B.C., Nguyen, T.M.-D., Weltrowska, G., Carpenter, K.A., Chung, N.N. and Schiller, P.W. (1998) J. Peptide Res. 51, 386–394, which was published during the course of our work.

[7] Molecular dynamics simulations in water show that PL-017 adopts an extended conformation.

Table 4
YPWF chemical shifts (ppm) in DMSO at 25°C

Peak	*trans*	*cis*
Y_{NH}	7.91 br	8.09 br
Y_{α}	4.126	3.442
$Y_{\beta1}$	2.681	2.746
$Y_{\beta2}$	2.838	2.746
$Y_{2,6}$	7.055	6.826
$Y_{3,5}$	6.623	6.601
Y_{OH}	9.282	9.346
P_{α}	4.321	3.572
$P_{\beta1}$	1.599	β: 1.522
$P_{\beta2}$	1.900	γ1: 1.383
P_{γ}	1.679	γ2: 1.458
$P_{\delta1}$	3.005	3.173
$P_{\delta2}$	3.522	3.300
W_{NH}	7.923	8.157
W_{α}	4.353	4.476
$W_{\beta1}$	2.886	2.860
$W_{\beta2}$	3.009	3.018
W_1	10.720	10.656
W_2	7.060	6.983
W_4	7.504	7.518
W_5	6.906	6.929
W_6	6.977	7.005
W_7	7.233	7.268
F_{NH}	7.833	8.020
F_{α}	4.435	4.391
$F_{\beta1}$	2.761	2.753
$F_{\beta2}$	2.897	2.943
F_{ar}	two bands 7.192–7.152	7.146–7.093
F_{CT1}	7.027	7.043
F_{CT2}	7.205	7.277

trans-Endomorphin-1 can also be compared with the NMR structure of the δ-agonist DPDPE, and a low energy conformation of δ-antagonist TIPP-NH_2. A molecular graphics overlay is given in Fig. 7. A comparison of the φ, ψ and χ_1 values for all of the peptides studied are shown in Table 3.

For DPDPE, the μ-selectivity region is not occupied, whereas the δ-activity region is. TIPP-NH_2 on the other hand possessed a low energy conformation which is capable of filling both the μ-selectivity pocket, as well as the δ-selectivity region. Interestingly, TIPP-NH_2 exhibits a dual μ-agonist/δ-antagonist profile [18].

Differentiation between the μ- and δ-selective ligands can be seen in the region of the C-terminus. Those of μ-ligands, which tend to be amidated, point up and away from the molecule and occupy a region which is distinctly separated from that occupied by the δ-ligands. On the other hand, the C-terminus of the δ-ligands (which tend to be free acids) occupies a region slightly lower in the putative receptor pocket. Schiller et al. have demonstrated that the δ-selectivity of TIPP-NH_2 can be increased dramatically if the C-terminal amide is replaced by the free acid [18]. Our model places the free acid in the location occupied by the free acid for the δ-selective ligand DPDPE.

5. Conclusion

This study has presented a structural and comparative study of endomorphin-1 in an effort to understand the structural attributes that impart opioid binding and selectivity. Overall, the results provide fairly convincing evidence that the bioactive form of endomorphin-1 is in the *trans*, or extended form. While *cis*, or compact conformers have been identified from NMR studies of related YP-Ar, the results reported here indicate that such structure is only present in DMSO, and that endomorphin-1 is devoid of internal hydrogen bonds which are a prerequisite for reverse turn or *cis* stabilization. It is therefore unlikely that endomorphin-1 adopts a similar *cis*-conformation. The significance of the *trans*-isomer to peptide binding and selectivity was further investigated through structural comparisons with two other μ-selective peptides PL-017 and D-TIPP, as well as the δ-selective peptide DPDPE. As shown in Fig. 6, alignment of the Tyr residues of endomorphin-1, PL-017 and D-TIPP, also allows significant overlap in the aromatic residues flanking Pro. In terms of the 'message-address' concept forwarded by Portoghese et al. [45,46], this secondary element may represent the 'address' or site of selectivity for the μ-opioid receptor. This hypothesis is further supported by structural alignments of endomorphin-1 and the δ-agonist DPDPE, which show little or no overlap between the putative μ-selectivity and δ-selectivity regions of these peptides. Perhaps the most provocative result is seen in the structural comparison using the dual μ-agonist/δ-antagonist TIPP-NH_2. In this case, both the μ and δ 'addresses', as well as the tyramine moieties or opioid 'message' of endomorphin-1 and DPDPE can be aligned onto TIPP-NH_2 to form a consistent picture relating structure and selectivity. It is important to point out, however, that our results do not rule out the existence of other, relevant conformations of endomorphin-1 to opioid binding, e.g. extended *cis*-conformations. Nevertheless, the results and analyses reported here should provide new insight to the development of a wide range of experimental and theoretical studies aimed at understanding the structural basis for ligand recognition and selectivity of opioid receptors, as well as the structure-function relationships of the endomorphins and other related ligands. For instance, site directed mutagenesis experiments, coupled with receptor docking studies of *trans*-endomorphin-1, may provide conclusive evidence as to the existence of a μ-opioid 'address' that, to date, has escaped detection. Such information may prove key in designing novel, highly selective μ compounds that may have value clinically and as pharmacological tools.

Acknowledgements: We thank Dr. Kenway Hoey and Ms. Anita Everson for the synthesis of the endomorphin-1 required for these studies. DMF acknowledges support from NIDA/NIH. Supporting information available: ROESY and NOESY spectra are available. In addition, all aspects of the molecular dynamics simulations and structures are available upon request.

Appendix

Supplementary material to Table 1 is given in Table 4.

References

[1] Dhawan, B.N., Cesselin, F., Raghubir, R., Reisine, T., Bradley, P.B., Portoghese, P.S. and Hamon, M. (1996) Pharmacol. Rev. 48, 567–592.
[2] Shahabi, N.A. and Sharp, B.M. (1995) J. Pharmacol. Exp. Ther. 273, 1105–1113.
[3] Sharp, B.M., Shahabi, N.A., Heagy, W., McAllen, K., Bell, M., Huntoon, C. and McKean, D.J. (1996) Proc. Natl. Acad. Sci. USA 93, 8294–8299.
[4] Lendvai, B., Sandor, N.T. and Sandor, A. (1993) Acta Physiol. Hung. 81, 19–28.

[5] Suzuki, T., Mori, T., Tsuji, M., Misawa, M. and Nagase, H. (1997) Eur. J. Pharmacol. 331, 1–8, and references cited therein.
[6] Huang, P. and Loew, G. (1997) J. Comp.-Aided Mol. Des. 11, 21–28.
[7] Fang, X., Larson, D.L. and Portoghese, P.S. (1997) J. Med. Chem. 40, 3064–3070.
[8] Portoghese, P.S. (1996) in: Perspective in Receptor Research (Giardina, D., Piergentili, A. and Pigini, M., Eds.), pp. 303–312, Elsevier Science, Amsterdam.
[9] Metzger, T.G. and Ferguson, D.M. (1995) FEBS Lett. 375, 1–4.
[10] Varga, E.V., Li, X., Stropova, D., Zalewska, T., Landsman, R.S., Knapp, R.J., Malatynska, E., Kawai, K., Mizusura, A., Nagase, H., Calderon, S.N., Rice, K., Hruby, V.J., Roeske, W.R. and Yamamura, H.I. (1996) Mol. Pharmacol. 50, 1619–1624.
[11] Hruby, V.J., Koa, L.-F., Pettitt, B.M. and Karplus, M. (1988) J. Am. Chem. Soc. 110, 3351–3359.
[12] Lomize, A.L., Pogozheva, I.D. and Mosberg, H.I. (1996) Biopolymers 38, 221–234.
[13] Paterlini, G., Portoghese, P.S. and Ferguson, D.M. (1997) J. Med. Chem. 40, 3263–3270.
[14] Tessmer, M.R., Meyer, J.-P., Hruby, V.J. and Kallick, D.A. (1997) J. Med. Chem. 40, 2148–2155.
[15] Flippen-Anderson, J.L., Deschamps, J.R., George, C., Reddy, P.A., Lewin, A.H., Brine, G.A., Sheldrick, G. and Nikiforovich, G. (1997) J. Peptide Res. 49, 384–393.
[16] Zadina, J.E., Hackler, L., Ge, L.-J. and Kastin, A.J. (1997) Nature 383, 499–502.
[17] Chang, K.J., Killian, A., Hazum, E., Cuatrecasas, P. and Chang, J.K. (1981) Science 212, 75–77.
[18] Schiller, P.W., Nguyen, T.M.-D., Weltrowska, G., Wilkes, B.C., Marsden, B.J., Lemieux, C. and Chung, N.N. (1992) Proc. Natl. Acad. Sci. USA 89, 11871–11875.
[19] Shaka, A.J., Lee, C.J. and Pines, A. (1988) J. Magn. Reson. 77, 274–293.
[20] Bax, A. and Davis, D. (1985) J. Magn. Reson. 65, 355–360.
[21] van Zijl, P.C.M., O'Neil-Johnson, M., Mori, S. and Hurd, R.E. (1995) J. Magn. Reson. A 113, 265–270.
[22] Sklenar, V., Piotto, M., Leppik, R. and Saudek, V. (1993) J. Magn. Reson. A 102, 241–245.
[23] Jeener, J., Meier, B.H., Bachmann, P. and Ernst, E.E.J. (1979) Chem. Phys. 71, 4546–4556.
[24] Bothner-By, A.A., Stephens, B.L., Lee, J., Warren, C.D. and Jeanloz, R.W. (1984) J. Am. Chem. Soc. 106, 811–813.
[25] Desvaux, H., Berthault, P., Birlirakis, N., Goldman, M. and Piotto, M. (1995) J. Magn. Reson. A 113, 47–52.
[26] Braunschweiler, L. and Ernst, R.R. (1983) Magn. Reson. 53, 521–528.
[27] Marion, D., Ikura, M., Tschudin, R. and Bax, A. (1985) J. Magn. Reson. 85, 393–399.
[28] Gasteiger, J. and Marsili, M. (1980) Tetrahedron 36, 3219–3228.
[29] Marsili, M. and Gasteiger, J. (1980) Croat. Chem. Acta 53, 601–614.
[30] Gasteiger, J. and Marsili, M. (1981) Organ. Magn. Reson. 15, 353–360.
[31] Streitwieser, A. (1961) Molecular Orbital Theory for Organic Chemists, Wiley, New York.
[32] Purcel, W.P. and Singer, J.A. (1967) J. Chem. Eng. Data 12, 235–246.
[33] Clark, M., Cramer III, R.D. and Van Opdenbosch, N. (1989) J. Comp. Chem. 10, 982–1012.
[34] Sybyl 6.0 Theory Manual, Appendix 2.2, pp. 2421–2423, October 1992.
[35] Demeter, D.A. (1994) Development and Application of Potential Energy Surface Analysis and the Local Minima Method of Pharmacophore Determiniation, Avail. Univ. Microfilms Int., Order No. DA9502554., 361 pp. From: Diss. Abstr. Int. B 1995, 55, 3896.
[36] Cramer III, R.D., Patterson, D.E. and Bunce, J.D. (1988) J. Am. Chem. Soc. 110, 5959–5967.
[37] Marshall, G. and Cramer III, R.D. (1988) Trends Pharmacol. Sci., 9, 285–289.
[38] Allen, M.S., Yan, Y.C., Trudell, M.L., Narayanan, K., Schindler, L.R., Martin, M.J., Schultz, C., Hagen, T.J., Koehler, K.F., Codding, P.W., Skolnick, P. and Cook, J.M. (1990) J. Med. Chem. 33, 2343–2357.
[39] Case, D.A., Pearlman, D.A., Caldwell, J.W., Cheatham, T.E., Ross, W.S., Simmerling, C.L., Darden, T.A., Merz, K.M., Stanton, R.V., Cheng, A.L., Vincent, J.J., Crowley, M., Ferguson, D.M., Radmer, R.J., Seibel, G.L., Singh, U.C., Weiner, P.K. and Kollman, P.A. (1997) AMBER 5, University of California, San Fransisco, CA.
[40] Wüthrich, K. (1986) NMR of Proteins and Nucleic Acids, John Wiley and Sons, New York.
[41] Yao, J., Dyson, J. and Wright, P.E. (1994) J. Mol. Biol. 243, 754–766.
[42] Roberts, V.A., Nachman, R.J., Coast, G.M., Hariharan, M., Chung, J.S., Holman, G.M., Williams, H. and Tainor, J.A. (1997) Curr. Biol. 4, 105–117.
[43] Temussi, P.A., Picone, D., Saviano, G., Amodeo, P., Motta, A., Tancredi, T., Salvadori, S. and Tomatis, R. (1992) Biopolymers 32, 367–372.
[44] Marshall, G.R., Barry, B.E., Bosshard, H.E., Dammkoehler, R.A. and Dunn, D.A. (1979) in: Computer Assisted Drug Design (Olson, E.C., Christofferson, R.E., Eds.), Vol. 112, pp. 205–226, ACS Symposium Series, Washington, DC.
[45] Takemori, A.E. and Portoghese, P.S. (1992) Annu. Rev. Pharmacol. Toxicol. 32, 239–269.
[46] Metzger, T.G., Paterlini, M.G., Portoghese, P.S. and Ferguson, D.M. (1996) Neurochem. Res. 21, 1287–1294.